Proportional-Integral-Resonant AC Current Controller

Djordje STOJIC[1], Tomasz TARCZEWSKI[2], Ilija KLASNIC[1]
[1]*Nikola Tesla Institute of Electrical Engineering, University of Belgrade, 11000 Belgrade, Serbia*
[2]*Institute of Physics, Nicolaus Copernicus University, 87-100 Torun, Poland*
djordje.stojic@ieent.org

***Abstract*—In this paper an improved stationary-frame AC current controller based on the proportional-integral-resonant control action (PIR) is proposed. Namely, the novel two-parameter PIR controller is applied in the stationary-frame AC current control, accompanied by the corresponding parameter-tuning procedure. In this way, the proportional-resonant (PR) controller, common in the stationary-frame AC current control, is extended by the integral (I) action in order to enable the AC current DC component tracking, and, also, to enable the DC disturbance compensation, caused by the voltage source inverter (VSI) nonidealities and by nonlinear loads. The proposed controller parameter-tuning procedure is based on the three-phase back-EMF-type load, which corresponds to a wide range of AC power converter applications, such as AC motor drives, uninterruptible power supplies, and active filters. While the PIR controllers commonly have three parameters, the novel controller has two. Also, the provided parameter-tuning procedure needs only one parameter to be tuned in relation to the load and power converter model parameters, since the second controller parameter is directly derived from the required controller bandwidth value. The dynamic performance of the proposed controller is verified by means of simulation and experimental runs.**

***Index Terms*—closed loop systems, control design, current control, induction motors, inverters.**

I. INTRODUCTION

AC current controllers represent a basis for various applications in small, mid, and large power range applications, including AC motor drives, uninterruptible power supplies, and active power filters. Depending on the particular application, dynamic performance requirements of the AC current controller may vary. Nevertheless, the AC current controllers need to enable: (i) asymptotic AC current reference tracking for variable reference frequencies and amplitudes; (ii) fast response speed determined by the application-specific requirements; (iii) compensation of both fundamental and higher harmonic disturbances related to different types of loads; (iv) compensation of the time delays introduced by current sampling and output voltage updating techniques, typical for the voltage source converters (VSC) based on the pulse width modulation (PWM); (v) control of the VSC switching frequency, in order to prevent the converter operation with the unacceptably high frequency values; and (vi) compensation of a DC disturbance introduced in the control loop by the VSC nonidealities and nonlinear loads.

In order to meet the outlined performance requirements several types of solutions have been proposed in the literature, which can be classified into two basic groups in [1-2]: nonlinear and linear controllers. The group of nonlinear solutions is represented by the hysteresis or bang-bang AC current controllers in [1]. Although it enables fast and very accurate reference tracking, the problem related to hysteresis control is that, if not managed, it can operate with variable and usually unacceptably high switching frequencies. However, hysteresis-based AC current controllers are proposed with adaptive hysteresis bands in [3-4] that can partially solve this problem.

Linear solutions can be classified into two major groups, stationary and synchronous-frame based solutions, represented by the following common types of controllers: (i) stationary-frame based PI controllers; (ii) stationary-frame proportional-resonant (PR) controllers, (iii) stationary-frame reduced order generalized integrator (ROGI) based controllers, (iv) stationary and synchronous-frame based controllers with the back-EMF compensation, (v) internal model control (IMC) based solutions, (v) predictive controllers, (vi) dead-beat controllers, (vii) state feedback based controllers, (viii) synchronous-frame based PI controllers, with or without the compensation of the coupling between the reference frame axes, and (ix) synchronous and stationary-frame based proportional-integral-resonant (PIR) controllers.

Stationary-frame based PI controllers in [5] represent the basic linear structure, used in both analog and digital implementations of linear AC current controllers. Namely, in [5], typical problems and corresponding solutions related to AC current controllers used with the three-phase back-EMF-type load are outlined: (i) the time delay related controller dynamic performance deterioration, (ii) the choice of the controller crossover frequency ω_I related to the PWM switching frequency and required phase margin values, and (iii) the modeling of the load and the VSI. Nevertheless, the main shortcoming of the stationary-frame based PI is that it does not enable asymptotic reference tracking.

Consequently, to overcome this obstacle, several different stationary-frame based solutions have been proposed, including the PR based controllers in [5–7], which enable asymptotic reference tracking. However, the lack of integral action in PR controller results in the fact that it is not able to compensate the DC current component, i.e., the DC disturbances introduced in the control loop by the nonideal VSI characteristics and nonlinear loads.

Similar to PR solutions, in [1, 8-9] reduced-order generalized integrator (ROGI) solutions are proposed, which represent the synchronous-frame based PI regulator

This work was supported by the Ministry of Education and Science of the Republic of Serbia.

Digital Object Identifier 10.4316/AECE.2017.01012

transformed into the stationary-frame.

In order to improve the reference tracking and DC disturbance compensation, for some types of three-phase loads (for example, for the induction motor) the stationary-frame PI controller based solutions in [6, 10] are extended by the back-EMF feed-forward compensation. In these cases, asymptotic reference tracking is enabled, which depends on the accurate induction motor stator flux estimation.

Together with the previous, there are several other application-specific AC current controllers: internal model control (IMC) based solutions in [11-12] that enable the asymptotic reference tracking; predictive in [13]; dead-beat in [14]; and state feedback-based controllers in [15].

Another way to achieve the asymptotic AC reference tracking, is represented by the synchronous-frame based PI controller in [1, 6], which operates with rotational reference frame synchronous with the application specific vector (usually, either stator or rotor flux vector). However, this solution exhibits the typical negative cross-coupling effect between the reference frame axes. Consequently, the synchronous-frame based PI controllers with cross-coupling compensation were introduced in [16-17]. Nevertheless, similarly to the stationary-frame based PR controllers, the synchronous-frame based PI controllers suffer from the fact that they are not able to compensate the DC disturbances that exist in the corresponding stationary-frame. In this and other similar cases, stationary-frame based DC disturbances can be minimized by introducing the "active resistance" technique in [18]. Also, several types of disturbances (for example, VSI voltage errors by current-sign-dependent interlocking) can be compensated by means of a corresponding feed-forward action.

The following group of solutions represents the proportional-resonant-integral (PIR) controllers in [19], commonly used in order to enable asymptotic DC reference tracking and to compensate AC disturbances with a known angular frequency. Namely, PIR controllers have so far been typically employed in the synchronous-frame based AC current control for the voltage source converters with the unbalanced voltage transients in [20].

However, there are papers dedicated to the stationary-frame based PIR controllers in [2, 21], and they are mainly oriented towards the application in utility-interface AC power converters: single phase in [21], and three-phase in [2]. However, in neither of these works the precise PIR controller parameter-tuning procedure is outlined, i.e., the controller parameter values were determined experimentally.

Finally, for both PR and PIR controllers it is necessary to define the resonant action discretization procedure, analyzed in [24]. Also, in [24] the compensation of time delay introduced in the control loop by current sampling and PWM updating is presented, designed for use with controllers that include the resonant action. In [25, 26] the compensated resonant controller applications are outlined, with the specific applications in active filters.

In this paper, an improved stationary-frame PIR controller is proposed for the AC current control in single or three-phase applications, ranging from utility-interface converters, AC motor drives, to uninterruptible power supplies with or without an output isolation transformer. When compared to the existing stationary-frame based PIR controllers, the novel controlling structure enables operation with a reduced set of control parameters, accompanied with the corresponding parameter-tuning procedure.

Namely, the common PIR controllers require three parameters to be tuned in relation to the VSI and load model parameters, while the new PIR controller effectively needs only one parameter to be tuned in relation to the VSI and load parameters, since the second controller parameter is directly proportional to the required bandwidth value.

This paper consists of six sections. In Section II the model of the back-EMF type three-phase load is presented, since various types of different loads can be approximated by this type of model. In Section III the new type of PIR controller is presented, together with the corresponding parameter-tuning procedure. In Section IV the simulation results of the proposed controller are presented, for the case of the three-phase induction motor used as the load. In Section V the experimental results are presented that correspond to the simulation tests presented in the Section IV. In Section VI, concluding remarks are presented.

II. Model of Back-EMF Type Three-Phase Load

The AC current controller proposed in this paper is developed for use in applications that can be modeled by means of back-EMF-type load in [1, 5], which include active filters, AC motor drives, uninterruptible power supplies, and various other types of AC power supplies. This type of load can be represented by the series impedance with the back-EMF, i.e., with the corresponding harmonic AC disturbance:

$$\begin{aligned} V_r &= R_e I_r + L_e \frac{\mathrm{d}}{\mathrm{dt}} I_r + e_r \\ V_s &= R_e I_s + L_e \frac{\mathrm{d}}{\mathrm{dt}} I_s + e_s \\ V_t &= R_e I_t + L_e \frac{\mathrm{d}}{\mathrm{dt}} I_t + e_t \end{aligned} \tag{1}$$

where V_r, V_s and V_t represent three-phase stationary-frame voltage components, I_r, I_s and I_t stationary-frame current components, and e_r, e_s and e_t stationary-frame back-EMF components. Also, R_e and L_e represent the resistance and inductance values of the back-EMF type load equivalent series impedance, represented in the following Fig. 1.

Furthermore, from (1) the following set of equations is obtained in $\alpha\beta$ stationary-frame:

$$\begin{aligned} V_\alpha &= R_e I_\alpha + L_e \frac{\mathrm{d}}{\mathrm{dt}} I_\alpha + e_\alpha \\ V_\beta &= R_e I_\beta + L_e \frac{\mathrm{d}}{\mathrm{dt}} I_\beta + e_\beta \end{aligned} \tag{2}$$

Finally, after introducing the complex variables $\underline{V} = V_\alpha + jV_\beta$, $\underline{I} = I_\alpha + jI_\beta$, and $\underline{e} = e_\alpha + je_\beta$ the following load model is obtained

$$\underline{V} = R_e \underline{I} + L_e \frac{\mathrm{d}}{\mathrm{dt}} \underline{I} + \underline{e} \tag{3}$$

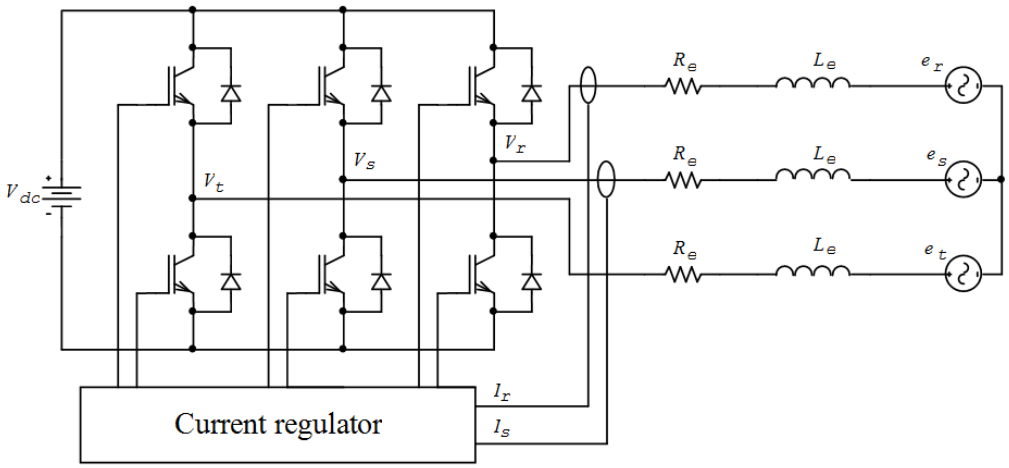

Figure 1. PWM-controlled voltage source inverter with the AC current control of back-EMF type three-phase load

However, together with the load model (3), it is necessary to define the PWM controlled three-phase VSI model. Namely, for the $\underline{V}_c$ representing the controller output operating in the range [-1, 1], the VSI can be represented by the transfer function $G_{VSI}(s) = K_{VSI}\, e^{(-sTd)}$. The VSI gain K_{VSI} is calculated from the inverter DC bus voltage V_{dc} (depicted in Fig. 1) as $K_{VSI} = V_{dc} / 2$. Also, the time delay T_d that is included in the VSI model represents the delay introduced into the control loop by two factors in [5]: the current sampling and the VSI output voltage PWM updating techniques. For example, for the commonly used double PWM updating technique the introduced VSI time delay is equal to $T_d = 1.5 / f_s$, where f_s represents the current sampling frequency. In our paper, the single PWM updating technique is employed, with the symmetric PWM and current sampling in the middle of the PWM signal, which introduces time delay $T_d = 1 / f_s$.

Consequently, the complete back-EMF type load model, used for the AC current controller design, based on (3) and on the VSI transfer function $G_{VSI}(s)$, is represented by:

$$\underline{I}(s) = \underline{V}_c(s)\frac{G_{VSI}(s)}{sL_e + R_e} - \frac{\underline{e}(s)}{sL_e + R_e} = \underline{V}_c(s)\frac{K_{VSI}\, e^{-sTd}}{sL_e + R_e} - \frac{\underline{e}(s)}{sL_e + R_e} \quad (4)$$

, where $\underline{V}_c$ represents the normalized AC current controller output, $K_{VSI} = V_{DC} / 2$, and $T_d = 1 / f_s$. Furthermore, for the single phase load a similar equation can be used, with the scalar variables used in (4) instead of the complex. Consequently, based on equation (4), for the back-EMF type three-phase load the back-EMF signal e is considered to be the AC disturbance with the same angular frequency ω_e as the AC current reference signal.

In the following section the new and improved version of the stationary-frame based PIR controller is presented, together with the corresponding parameter-tuning procedure.

III. Stationary-Frame Based PIR Controller

The novel AC current controller proposed in this paper belongs to the group of the stationary-frame based sequential controllers, with the asymptotic reference tracking enabled by the means of a resonant control action. Namely, based on the three-phase load and VSI model (4) the outline of sequential AC current controller is presented in Fig. 2.

Commonly used PR sequential AC controller in [7] is represented by the following transfer function

$$G_{PR}(s) = K_P + K_R \frac{s}{s^2 + \omega_e^2} \quad (5)$$

, where ω_e represents the AC current reference angular frequency. The problem related to this type of controller is that it is not able to compensate the DC disturbance introduced into the control loop by nonlinear VSI characteristics in [24] or nonlinear loads. In [2, 21], the stationary-frame PIR controller (6) is proposed, which solves the aforementioned problem:

$$G_{PIR}(s) = K_P + K_I \frac{1}{s} + K_R \frac{s}{s^2 + \omega_e^2} \quad (6)$$

However, in [2, 21] the three-parameter K_P, K_I, and K_R controller (6) is proposed, with no parameter-tuning procedure. In our paper, the novel PIR structure (7) is proposed that has 2 parameters K_{PIR} and a_{PIR}. It is, also, accompanied by the corresponding parameter-tuning procedure, based on the plant model and on the required phase margin value.

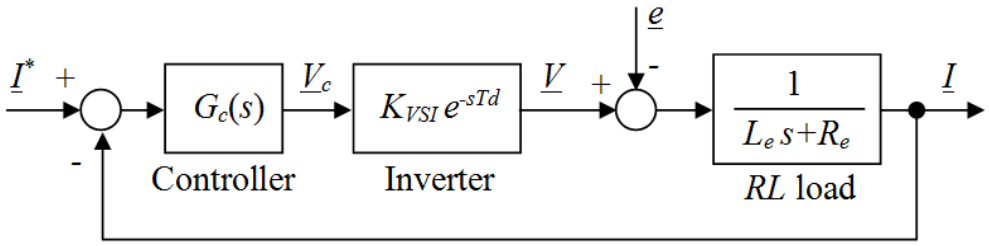

Figure 2. The AC current control loop with back-EMF type three-phase load

$$G_{PIR}(s) = K_{PIR}\frac{(s+a_{PIR})^3}{s(s^2+\omega_e^2)} \quad (7)$$

Based on Fig. 2, the following plant transfer function $G_{PL}(s)$ (8) can be derived, which is used in the controller parameter-tuning procedure.

$$G_{PL}(s) = \frac{K_{VSI}\,e^{-sTd}}{sL_e + R_e} \quad (8)$$

The parameter-tuning procedure is based on the required phase margin φ^*_{PM}, and on the time delay T_d (8), which is introduced into the control loop by current sampling and PWM updating techniques. Also, the controller (7) parameters are derived under the presumption that $\omega_1 > \omega_e$ *and* $\omega^2_1 >> \omega^2_e$ (where ω_1 represents the crossover frequency, and ω_e the reference frequency) for any chosen ω_e value, which is a common case in AC power converter applications.

In order to calculate K_{PIR} (7) the crossover frequency ω_1 needs to be determined, based on the condition that a_{PIR} is chosen to be 10% of ω_1, since in that case the overall contribution of G_{PIR} (7) to the phase margin is approximately equal to zero. Namely, this is accomplished for any $\omega_1 > \omega_e$, which is the common case in AC current controllers. In that case the phase margin is approximated by

$$\varphi_{PM} \geq \pi/2 - \omega_1 T_d \ , \quad (9)$$

for any values of ω_e. R_e and L_e. From (9), equations (10) and (11) are obtained. These are used to calculate the reference crossover frequency ω_1 and a_{PIR} from the given phase margin value φ^*_{PM} (which should not exceed $\pi/2$),

$$\omega_1 = \frac{\pi/2 - \varphi^*_{PM}}{T_d} \quad (10)$$

$$a_{PIR} = \omega_1/10 \quad (11)$$

However, if from equation (10) an insufficient crossover frequency ω_1 value is obtained (which corresponds to the bandwidth frequency of the particular AC current controller application), the smaller phase margin value φ^*_{PM} needs to be adopted, and controller design steps (10) and (11) correspondingly repeated. Based on (10) and (11) and by neglecting T_d, the following K_{PIR} equation (12) is obtained

$$K_{PIR} \approx \frac{\omega_1(\omega_1^2-\omega_e^2)\sqrt{\omega_1^2L_e^2+R_e^2}}{K_{VSI}\left(\sqrt{\omega_1^2+a_{PIR}^2}\right)^3} \approx \frac{(\omega_1^2-\omega_e^2)\sqrt{\omega_1^2L_e^2+R_e^2}}{\omega_1^2 K_{VSI}} \quad (12)$$

, for $a_{PIR} = \omega_1/10$ and $\omega_e < \omega_1$.

For the case of AC current controllers where $\omega_e < \omega_1/3$, K_{PIR} can be approximated by

$$K_{PIR} \approx \frac{\sqrt{\omega_1^2L_e^2+R_e^2}}{K_{VSI}} \quad (13)$$

Consequently, equations (10) to (13) represent the novel PIR controller (7) two-parameter-tuning procedure, which shows that only one parameter K_{PIR} (12) effectively needs to be tuned in relation to the VSI and load parameters, while parameter a_{PIR} (11) is directly calculated from the required crossover frequency value, i.e., from the required phase margin value.

Since the AC disturbance for the fundamental component is compensated by means of the resonant action included in the controller, the higher harmonic disturbances can further be minimized by means of the "active resistance" technique in [18] that represents a local current feedback action K_A, depicted in Fig 3.

Regarding the parameter-tuning procedure, in the case when the "active resistance" action is applied, equations (10) and (11) remain the same. The choice of K_{PIR} is approximated by the equation (14), by neglecting T_d.

$$K_{PIR} \approx \frac{\sqrt{\omega_1^2L_e^2+(R_e+K_AK_{VSI})^2}}{K_{VSI}} \quad (14)$$

, for $a_{PIR} = \omega_1/10$ and for $\omega_e < \omega_1/3$.

In the following section, the novel PIR AC current controller is examined by means of simulations, with an induction motor used as a three-phase load.

IV. Simulations

In this section an induction motor is used as the three-phase AC current controller load. The complex variable vector based IM motor model in [10] can be represented by

$$\begin{aligned} \underline{V}_s(s) &= R_s\underline{I}_s(s) + s\underline{\psi}_s(s) \\ 0 &= R_r\underline{I}_r(s) + s\underline{\psi}_r(s) - j\omega_r\underline{\psi}_r(s) \\ \underline{\psi}_s(s) &= (L_{ls}+L_m)\underline{I}_s(s) + L_m\underline{I}_r(s) \\ \underline{\psi}_r(s) &= (L_{lr}+L_m)\underline{I}_r(s) + L_m\underline{I}_s(s) \end{aligned} \quad (15)$$

, where $\underline{V}_s$, $\underline{I}_s$, $\underline{\psi}_s$ and $\underline{\psi}_s$ represent stator voltage, stator current, stator flux, and rotor flux complex vectors, respectively. Also, R_s, R_r, L_m, L_{ls}, and L_{lr} represent IM stator resistance, rotor resistance, magnetizing inductance, stator leakage inductance, and rotor leakage inductance, respectively.

However, in [5] it is shown that the IM model can be approximated by the equivalent back-EMF-type load in the form of eq. (3), for $R_e = R_s$ and for (16).

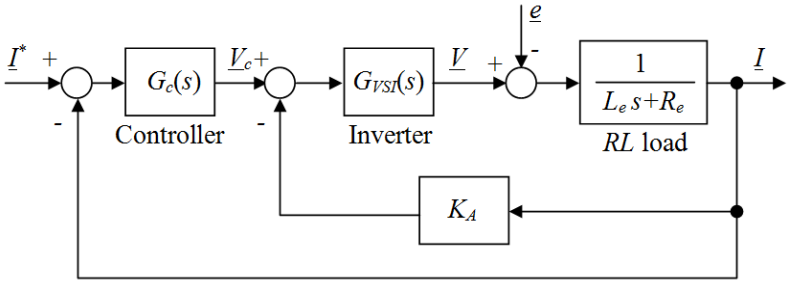

Figure 3. AC current control loop with "active resistance" control action

$$L_e = L_{ls} + \frac{L_{lr} L_m}{L_{lr} + L_m} \tag{16}$$

Consequently, based on this IM model approximation, the PIR controller (7) is used to control the IM stator current in different motor drive applications. In our case, the IM model has the following parameters: R_s = 8.6 Ω, R_r = 5.1 Ω, L_m = 0.381 H, L_{ls} = 0.008 H, and L_{lr} = 0.009 H, with a pole-pair number of 1. The VSI has K_{vsi} = 160 and $T_d = 1T_s$, where T_s represents the stator current control system sampling period T_s = 200 μs, with the single PWM updating (T_{PWM} = 200 μs). Hence, based on (10)–(12) and for a phase margin value φ^*_{PM} = 70° from [10] the following set of PIR controller parameters is obtained: K_{PIR} = 0.19 and a_{PIR} = 174 rad/s, with the crossover frequency value (10) equal to ω_l = 1745 rad/s.

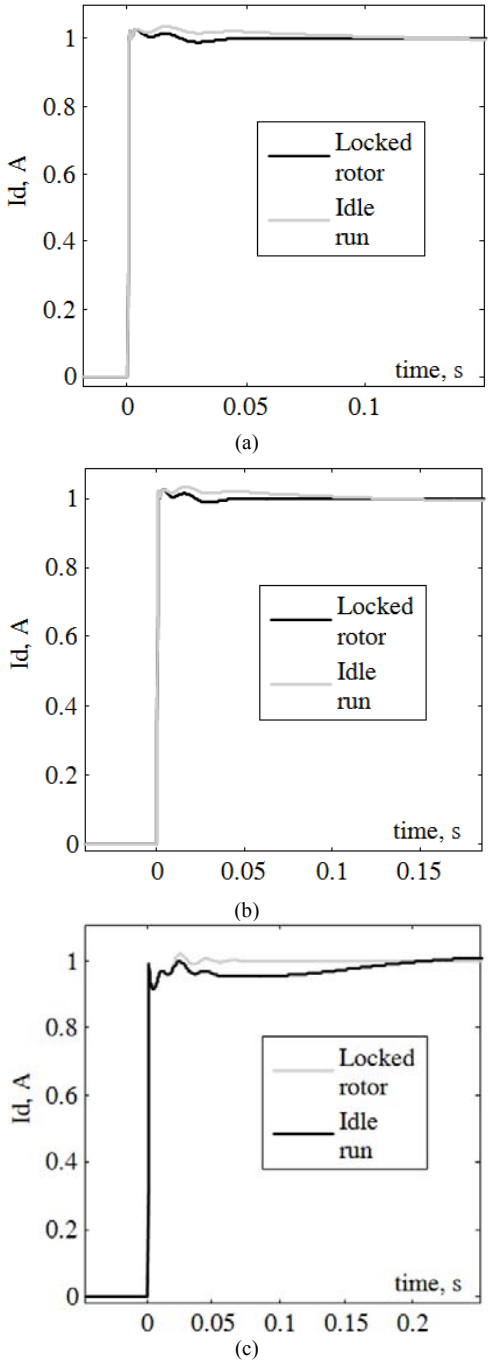

Figure 4. Stator current I_d component for locked rotor and motor in the idle run (a) $\omega_e = 2\pi5$ rad/s, (b) $\omega_e = 2\pi25$ rad/s, and (c) $\omega_e = 2\pi50$ rad/s

Furthermore, in the following simulation tests, the IM AC stator current responses are transformed into the rotational reference frame synchronous with the stator voltage in order to enable a more detailed insight in the current controller dynamics. In Fig. 4 the step responses of the stator-current component I_d are given for three different stator voltage frequencies, $\omega_e = 2\pi5$ rad/s, $\omega_e = 2\pi25$ rad/s, and $\omega_e = 2\pi50$ rad/s, for the locked rotor and for the motor in idle run. As I_d current reference signal step changes from 0 A to 1 A were used.

By analyzing the stator-current responses in Fig. 4 the following can be concluded: (i) the overshoot of 2% corresponds to the phase margin value equal to φ_{PM} = 70°; (ii) the response rising time t_r = 1.3 ms corresponds to crossover frequency equal to ω_l = 1754 rad/s, since $t_r \approx 2\pi0.35/\omega_l$; (iii) the proposed controller is robust in relation to variations of the stator frequency ω_e and rotor speed ω_r, since the response overshot and rising time vary over a small range for significant variations of ω_e and ω_r,.

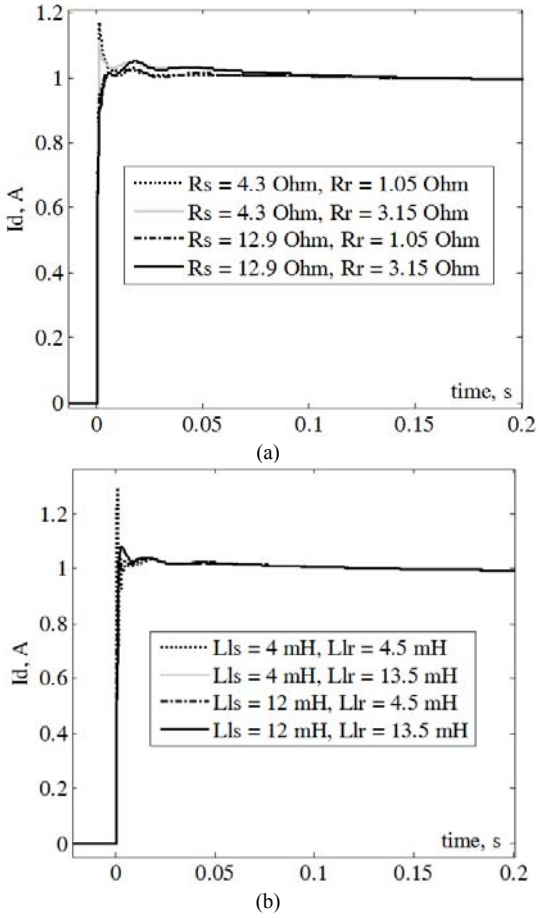

Figure 5. Stator current I_d component for locked rotor and $\omega_e = 2\pi25$ rad/s for (a) R_s and R_r varying in ±50% range and (b) L_{ls} and L_{lr} varying in ±50% range

In Fig. 5(a) the current responses are presented for stator and rotor resistances varying in the ±50% range, for ω_e = $2\pi25$ rad/s and ω_r = 0 rad/s. Furthermore, in Fig. 5(b) the stator-current responses are presented for L_{ls} and L_{lr} varying in the ±50% range (namely, based on (17) it can be concluded that the equivalent load inductance L_e predominantly depends on L_{ls} and L_{lr}, since $L_m >> L_{ls}$ and $L_m >> L_{lr}$). Based on the step responses it can be concluded that the controller retains the designed response speed for a wide

range of IM model parameter variations.

In the following section, the results of experimental tests are presented. The experimental setup is implemented by using the induction motor as a three-phase load.

V. Experimental Tests

Experimental tests were performed, based on the setup with the one-pole-pair, 1 kW, 220 V, 50 Hz induction motor, and with the control section consisting of: (a) control card running the real-time control software (reference generation and stator current control) operating with the f_s = 5 kHz sampling frequency, with the single PWM updating mode; (b) protection electronics; (c) current transducers; (d) IGBT drivers; and (e) three-phase IGBT VSI operating at 5 kHz switching frequency used for the IM stator current control.

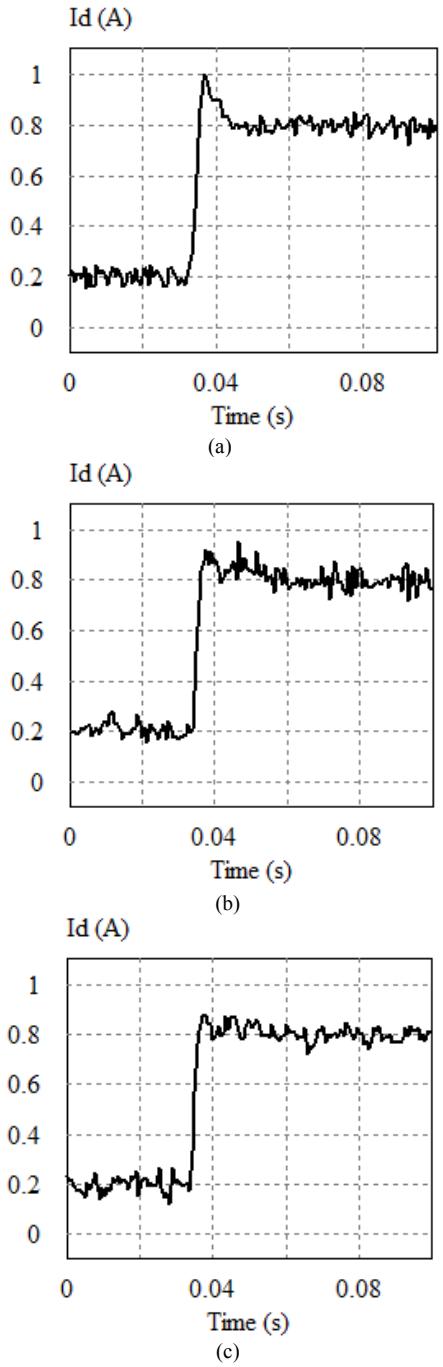

Figure 6. Stator current step responses for locked rotor (a) $\omega_e = 2\pi 5$ rad/s, (b) $\omega_e = 2\pi 25$ rad/s, and (c) $\omega_e = 2\pi 50$ rad/s

The set of controller parameters has been given in Section IV: K_{PIR} = 0.19, a_{PIR} = 174 rad/s, and K_A = 0, which correspond to φ^*_{PM} = 70º. Also, the set of IM model parameters has been given in Section IV.

In Fig. 6. the step responses of the stator-current component I_d are presented for a stator-current I_d reference step change from 0.2 A to 0.8 A, I_q = 0, three different ω_e values, and for locked rotor (ω_r = 0 rad/s). By analyzing the stator-current step responses it can be concluded that they correspond to the results presented in Section IV – the stator current rising time is close to 1.35 ms in all three cases, with slight increase in overshot value for $\omega_e = 2\pi 5$ rad/s. In this way the robustness in relation to the variable stator excitation frequency values is confirmed.

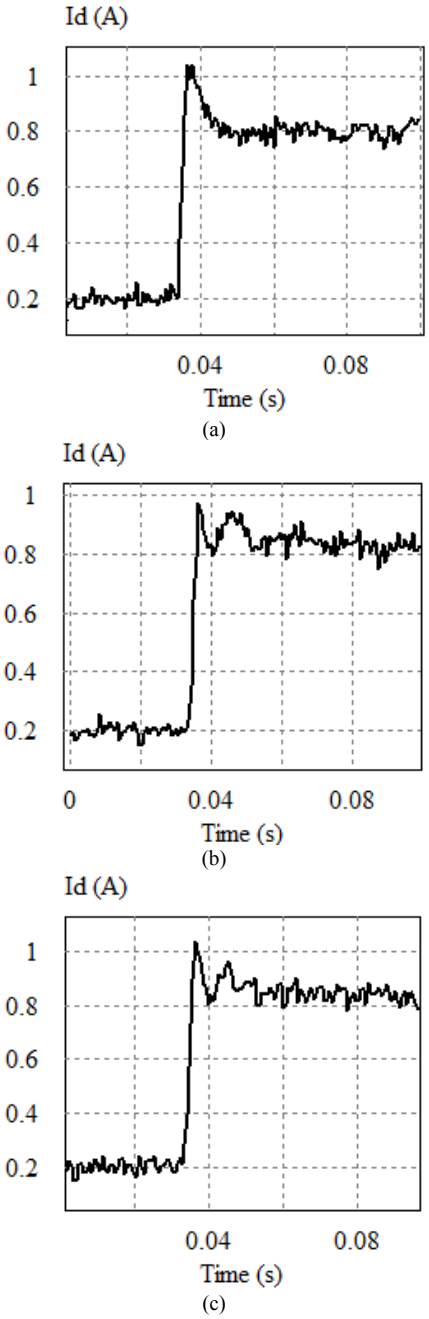

Figure 7 Stator current step responses for motor in the idle run (a) $\omega_e = 2\pi 5$ rad/s, (b) $\omega_e = 2\pi 25$ rad/s, and (c) $\omega_e = 2\pi 50$ rad/s

In Fig. 7 the stator current responses are given for IM in an idle run, i.e., for rotor running at subsynchronous speed, for (a) $\omega_e = 2\pi 5$ rad/s, (b) $\omega_e = 2\pi 25$ rad/s, and for (c) ω_e =

$2\pi 50$ rad/s. By analyzing the stator-current step responses it can be concluded that the stator current controller operation does not change significantly when compared to the performance with the locked rotor. Also, it can be concluded that all three responses in Fig. 7 exhibit an increased overshoot values, when compared to corresponding simulation results in Fig. 4.

In order to examine the influence of the integral action in the novel PIR current controller, in Fig. 8 the I_r stator current responses are presented for $\omega_e = 2\pi 25$ rad/s with locked rotor, for (a) PR controller (5) and (b) PIR controller (7), with the DC component of 10 V added to the V_r stator voltage. The DC disturbance is added in order to emulate the VSI dead-time value inconsistencies, or some other type of VSI nonlinearity.

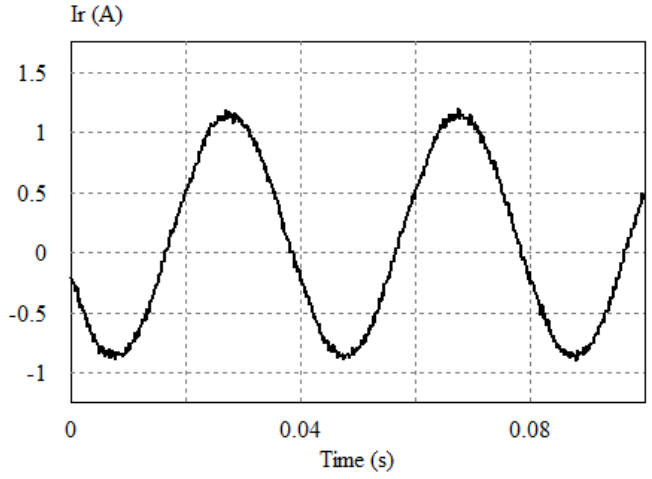

Figure 8. The I_r responses for $\omega_e = 2\pi 25$ rad/s with locked rotor and 10 V DC disturbance at V_r for (a) PR controller (5) and (b) PIR controller (7)

By analyzing the I_r current responses it can be concluded that PR controller (5) cannot compensate a DC disturbance, in contrast to PIR (7), which can. This difference can be critical in various AC current controller applications – i.e. IM drives, or AC power converters with an output isolation transformer.

VI. Conclusion

In this paper, a novel stationary-frame based AC current controller has been presented, based on the PIR structure. An improved controller was proposed, which enables AC current control with asymptotic AC reference tracking and DC disturbance compensation that is introduced by the nonidealities of the power converter stage and by the nonlinear loads. In this way, when compared to the stationary-frame-based PR or the synchronous-frame-based PI controllers, the novel controller enables the stationary-frame-based DC-component regulation, which can be critical in various AC current controller applications – for example, IM drives, or uninterruptable power supplies. Also, when compared to existing stationary-frame based PIR controllers, the novel controller introduces the following improvements: new structure with a reduced set of 2 parameters, and the corresponding parameter-tuning procedure. The parameter-tuning procedure is based on the equivalent three-phase RL load time constant, and on the required control system phase margin and crossover frequency values. Also, in the paper a modification of the basic solution is proposed, which consists of the controller supported by the "active resistance" feedback term. In this way, the disturbance rejection is improved, which can be useful in the case of the disturbances with higher frequency. The controller performance was examined through a series of simulation and experimental runs. Simulation runs consist of stator current responses for different excitation frequencies with the motor in locked state and idle run. In the experimental runs, the similar set of tests is performed, verifying the improved level of the controller dynamic performance.

References

[1] M. P. Kazmierkowski and L. Malesani, "Current control techniques for three-phase voltage-source PWM converters: a survey," Industrial Electronics, IEEE Transactions, vol. 45, pp. 691–703, 1998. doi: 10.1109/41.720325

[2] S. Fukuda and R. Imamura, "Application of a sinusoidal internal model to current control of three - phase utility interface converters," Electrical Engineering in Japan, vol. 150, pp. 54–61, 2005. doi: 10.1002/eej.20064

[3] S. Buso, S. Fasolo, L. Malesani, and P. Mattavelli, "A dead-beat adaptive hysteresis current control," Industry Applications, IEEE Transactions, vol. 36, pp. 1174–1180, 2000. doi: 10.1109/28.855976

[4] D. G. Holmes, R. Davoodnezhad, and B. P. McGrath, "An improved three-phase variable-band hysteresis current regulator," Power Electronics, IEEE Transactions, vol. 28, pp. 441–450, 2013. doi: 10.1109/tpel.2012.2199133

[5] D. G. Holmes, T. A. Lipo, B. P. McGrath, and W. Y. Kong, "Optimized design of stationary frame three phase AC current regulators," Power Electronics, IEEE Transactions, vol. 24, pp. 2417–2426, 2009. doi: 10.1109/tpel.2009.2029548

[6] D. G. Holmes, B. P. McGrath, and S. G. Parker, "Current regulation strategies for vector-controlled induction motor drives," Industrial Electronics, IEEE Transactions, vol. 59, pp. 3680–3689, 2012. doi: 10.1109/tie.2011.2165455

[7] D. N. Zmood and D. G. Holmes, "Stationary frame current regulation of PWM inverters with zero steady-state error," Power Electronics, IEEE Transactions, vol. 18, pp. 814–822, 2003. doi: 10.1109/tpel.2003.810852

[8] T. M. Rowan and R. J. Kerkman, "A new synchronous current regulator and an analysis of current-regulated PWM inverters," Industry Applications, IEEE Transactions, vol: IA-22, pp. 678–690, 1986. doi: 10.1109/tia.1986.4504778

[9] C. A. Busada, S. Gomez Jorge, A. E. Leon, and J. A. Solsona, "Current controller based on reduced order generalized integrators for distributed generation systems," Industrial Electronics, IEEE Transactions, vol. 59, pp. 2898–2909, 2012. doi: 10.1109/tie.2011.2167892

[10] D. M. Stojic, M. Milinkovic, S. Veinovic, and I. Klasnic, "Stationary Frame Induction Motor Feed Forward Current Controller With Back EMF Compensation," Energy Conversion, IEEE Transactions, vol. PP, pp. 1–11, 2015. doi: 10.1109/tec.2015.2438093

[11] L. Harnefors and H. P. Nee, "Model-based current control of AC machines using the internal model control method," Industry

Applications, IEEE Transactions, vol. 34, pp. 133–141, 1998. doi: 10.1109/28.658735

[12] A. Petersson, L. Harnefors, and T. R. Thiringer, "Evaluation of current control methods for wind turbines using doubly-fed induction machines," Power Electronics, IEEE Transactions, vol. 20, pp. 227–235, 2005. doi: 10.1109/tpel.2004.839785

[13] L. Zhang, R. Norman, and W. Shepherd, "Long-range predictive control of current regulated PWM for induction motor drives using the synchronous reference frame," Control Systems Technology, IEEE Transactions, vol. 5, pp. 119–126, 1996. doi: 10.1109/87.553670

[14] S. M. Yang and C. H. Lee, "A deadbeat current controller for field oriented induction motor drives," Power Electronics, IEEE Transactions, vol. 17, pp. 772–778, 2002. doi: 10.1109/tpel.2002.802182

[15] R. D. Lorenz and D. B. Lawson, "Performance of feedforward current regulators for field-oriented induction machine controllers," Industry Applications, IEEE Transactions, pp. 597–602, 1987. doi: 10.1109/tia.1987.4504956

[16] J. Jung and K. Nam, "A dynamic decoupling control scheme for high-speed operation of induction motors," Industrial Electronics, IEEE Transactions, vol. 46, pp. 100–110, 1999. doi: 10.1109/41.744397

[17] B. Bahrani, S. Kenzelmann, and A. Rufer, "Multivariable-PI-based current control of voltage source converters with superior axis decoupling capability," Industrial Electronics, IEEE Transactions, vol. 58, pp. 3016–3026, 2011. doi: 10.1109/tie.2010.2070776

[18] L. Harnefors, K. Pietilainen, and L. Gertmar, "Torque-maximizing field-weakening control: design, analysis, and parameter selection," Industrial Electronics, IEEE Transactions, vol. 48, pp. 161–168, 2001. doi: 10.1109/41.904576

[19] M. Ruderman and T. Bertram, "Variable proportional-integral-resonant (PIR) control of actuators with harmonic disturbances," Mechatronics (ICM), 2013 IEEE International Conference, pp. 847–852, 2013. doi: 10.1109/icmech.2013.6519151

[20] I. Etxeberria-Otadui, U. Viscarret, M. Caballero, A. Rufer, and S. Bacha, "New optimized PWM VSC control structures and strategies under unbalanced voltage transients," Industrial Electronics, IEEE Transactions, vol. 54, pp. 2902–2914, 2007. doi: 10.1109/tie.2007.901373

[21] S. Fukuda and T. Yoda, "A novel current-tracking method for active filters based on a sinusoidal internal model [for PWM invertors]," Industry Applications, IEEE Transactions, vol. 37, pp. 888–895, 2001. doi: 10.1109/28.924772

[22] J. Holtz and J. Quan, "Sensorless vector control of induction motors at very low speed using a nonlinear inverter model and parameter identification," Industry Applications, IEEE Transactions, vol. 38, pp. 1087–1095, 2002. doi: 10.1109/TIA.2002.800779

[23] A. G. Yepes, A. Vidal, J. Malvar, O. Lopez, and J. Doval-Gandoy, "Tuning method aimed at optimized settling time and overshoot for synchronous proportional-integral current control in electric machines," Power Electronics, IEEE Transactions, vol. 29, no. 6, pp. 3041–3054, 2014. doi: 10.1109/tpel.2013.227605

[24] Yepes, A.G., Freijedo, F.D., López, O. and Doval-Gandoy, J., "High-performance digital resonant controllers implemented with two integrators, " IEEE Transactions on Power Electronics, vol. 26,, pp.563-576, 2011. doi: 10.1109/tpel.2010.2066290

[25] C. Xia, B. Ji and Y. Yan, "Smooth Speed Control for Low-Speed High-Torque Permanent-Magnet Synchronous Motor Using Proportional–Integral–Resonant Controller," in IEEE Transactions on Industrial Electronics, vol. 62, pp. 2123-2134, 2015. doi: 10.1109/tie.2014.2354593

[26] A. Hasanzadeh, O. C. Onar, H. Mokhtari and A. Khaligh, "A Proportional-Resonant Controller-Based Wireless Control Strategy With a Reduced Number of Sensors for Parallel-Operated UPSs," in IEEE Transactions on Power Delivery, vol. 25, pp. 468-478, 2010. doi: 10.1109/tpwrd.2009.2034911